

## Appendix A

### Supplementary Information

# Silicon-Integrated Lead-Free BaTiO<sub>3</sub>-Based Film Capacitors with Excellent Energy Storage Performance and Highly Stable Irradiation Resistance

Fan Zhao,<sup>ab</sup> Yilin Wu,<sup>ab</sup> Yanzhu Dai,<sup>ab</sup> Guangliang Hu,<sup>ab</sup> Ming Liu,<sup>\*ab</sup> Runlong Gao,<sup>cd</sup> Linyue Liu,<sup>\*c</sup> Xin Liu,<sup>e</sup> Yonghong Cheng,<sup>\*e</sup> Tian-Yi Hu,<sup>b</sup> Chunrui Ma,<sup>b</sup> Dengwei Hu,<sup>f</sup> Xiaoping Ouyang<sup>c</sup> and Chun-Lin Jia<sup>abg</sup>

<sup>a</sup> School of Microelectronics, Xi'an Jiaotong University, Xi'an 710049, China

<sup>b</sup> State Key Laboratory for Mechanical Behavior of Materials, Xi'an Jiaotong University, Xi'an 710049, China

<sup>c</sup> State Key Laboratory of Intense Pulsed Radiation Simulation and Effect, Northwest Institute of Nuclear Technology, Xi'an 710024, China

<sup>d</sup> School of Nuclear Science and Technology, Xi'an Jiaotong University, Xi'an 710049, China

<sup>e</sup> State Key Laboratory of Electrical Insulation and Power Equipment, School of Electrical Engineering, Xi'an Jiaotong University, Xi'an 710049, China

<sup>f</sup> Faculty of Chemistry and Chemical Engineering, Engineering Research Center of Advanced Ferroelectric Functional Materials, Key Laboratory of Phytochemistry of Shaanxi Province, Baoji University of Arts and Sciences, 1 Hi-Tech Avenue, Baoji, Shaanxi, 721013 P. R. China

<sup>g</sup> Ernst Ruska Centre for Microscopy and Spectroscopy with Electrons, Forschungszentrum Jülich, D-52425 Jülich, Germany

---

\* Email address: [m.liu@xjtu.edu.cn](mailto:m.liu@xjtu.edu.cn); [13619269436@163.com](mailto:13619269436@163.com); [cyh@xjtu.edu.cn](mailto:cyh@xjtu.edu.cn)

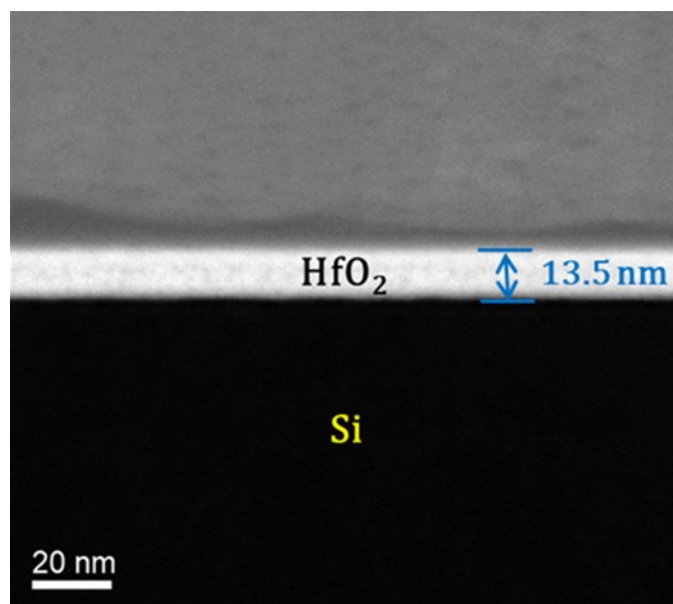


Fig. S1 A low-magnification dark field STEM image of an HfO<sub>2</sub> buffer layer deposited on Si substrate by atomic layer deposition technique.

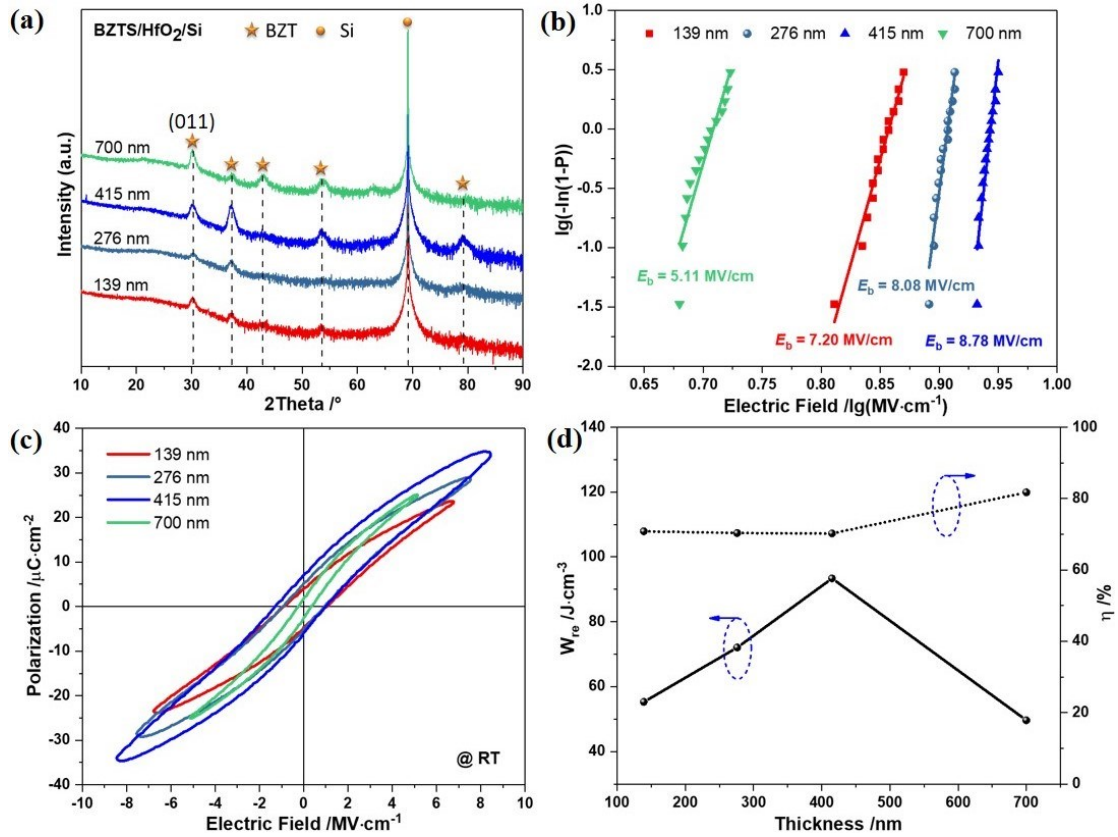


Fig. S2 (a) Typical XRD  $\theta$ - $2\theta$  scans of the BZTS/HfO<sub>2</sub> thin films with different thicknesses deposited on Si substrate. (b) The Weibull distribution and the fitting lines of  $E_b$  for the BZTS/HfO<sub>2</sub> thin films with different thicknesses. (c)  $P$ - $E$  hysteresis loops of the BZTS/HfO<sub>2</sub> thin films with different thicknesses. (d)  $W_{re}$  and  $\eta$  of the BZTS/HfO<sub>2</sub> thin films at room temperature depending on film thickness.

Fig. S2a shows the XRD  $\theta$ - $2\theta$  scans of the BZTS/HfO<sub>2</sub> thin films deposited on Si substrate with thicknesses of 139, 276, 415 and 700 nm. The results show that the BZTS/HfO<sub>2</sub> thin films of different thicknesses grown on the Si substrate also show perovskite-phase polycrystalline films. It can be seen from the Fig S2a that the diffraction intensity of the BZTS/HfO<sub>2</sub> films increases with increasing thickness, except for the BZTS/HfO<sub>2</sub> films with a thickness of 700 nm. At the same time, we also noticed that the sample with a thickness of 700 nm had a stronger (011) peak, which may be due to its stronger orientation. According to Eq. (1),  $E_b$  and  $P_{max} - P_r$  are the key parameters determining the  $W_{re}$  of dielectric capacitors. The fitting Weibull distribution of  $E_b$  of the BZTS/HfO<sub>2</sub> thin films with different thicknesses at RT are

shown in Fig. S2b. It can be seen that the  $E_b$  of the BZTS/HfO<sub>2</sub> thin films first increases and then decreases as the thickness increases. The nonmonotonic variation of  $E_b$  with film thickness may be attributed to the following reasons: First, we obtained the highest  $E_b$  value (about 8.78 MV/cm) in films with optimized thicknesses of ~415 nm.  $E_b$  decreases in thicker films because of the size effect [ $E_b \propto 1/\sqrt{\text{thickness}}$ ].<sup>1</sup> Secondly, when the film thickness exceeds a certain level, the contribution of the thinner HfO<sub>2</sub> buffer layer to the breakdown resistance of the film is relatively weak, which may lead to the decrease of  $E_b$ . Finally, it may be attributed to the fact that when the film exceeds a certain thickness, its crystalline quality deteriorates as the thickness increases and defects in the film increase, resulting in a decrease in  $E_b$ . Fig. S2c shows the  $P$ - $E$  loops of the BZTS/HfO<sub>2</sub> thin films with different thickness. The energy storage parameters of the BZTS/HfO<sub>2</sub> thin films obtained by  $P$ - $E$  loops integral calculation are summarized in Table S1. It can be seen that both  $P_{\max}$  and  $P_r$  increase first and then decrease with the increase of film thickness, and  $P_{\max} - P_r$  reaches the maximum value when the thickness is about 415 nm. Fig. S2d shows the change of  $W_{re}$  and  $\eta$  of the BZTS/HfO<sub>2</sub> thin films with the thickness. The results show that the change of  $W_{re}$  with thickness of the BZTS/HfO<sub>2</sub> thin films is consistent with that of  $E_b$  and  $P_{\max} - P_r$ . The ultrahigh  $W_{re}$  of 93.37 J/cm<sup>3</sup> with  $\eta$  of 70.22% at RT when the film thickness is about 415 nm is mainly due to its higher  $E_b$  and  $P_{\max} - P_r$ .

**Table S1**

Energy storage parameters of BZTS/HfO<sub>2</sub> thin films with different thickness grown on Si substrate at room temperature

Thickness /nm	$E_b$ /MV·cm <sup>-1</sup>	$P_{\max}$ / $\mu$ C·cm <sup>-2</sup>	$P_r$ / $\mu$ C·cm <sup>-2</sup>	$W_{re}$ /J·cm <sup>-3</sup>	$\eta$ /%
139	7.20	23.65	4.01	55.32	70.83
276	8.08	28.89	5.14	72.08	70.33
415	8.78	34.78	7.07	93.37	70.22
700	5.11	24.96	1.81	49.67	81.73

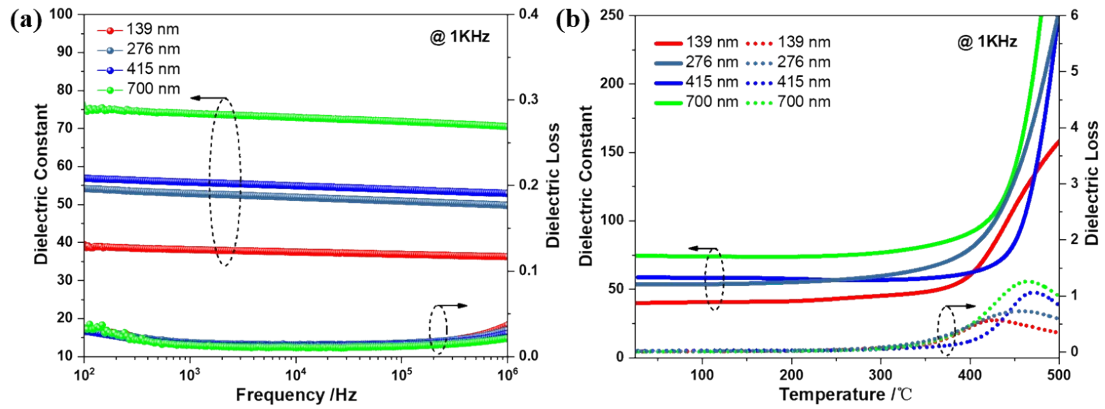


Fig. S3 (a) Frequency dependence of  $\epsilon_r$  and  $\tan\delta$  for the BZTS/HfO<sub>2</sub> thin films with different thicknesses at room temperature. (b) Temperature dependence of  $\epsilon_r$  and  $\tan\delta$  for the BZTS/HfO<sub>2</sub> thin films with different thicknesses at 1 KHz.

Fig. S3a shows the frequency dependence of  $\epsilon_r$  and  $\tan\delta$  for the BZTS/HfO<sub>2</sub> thin films with different thicknesses at RT. The results show that the  $\epsilon_r$  of the BZTS/HfO<sub>2</sub> thin films with different thickness decreases monotonously with the increase of frequency. This is mainly due to the polarization relaxation. The  $\epsilon_r$  of the BZTS/HfO<sub>2</sub> thin films gradually increases with the increase of the film thickness, which is mainly due to the influence of the interface layer with low dielectric constant on the BZTS/HfO<sub>2</sub> thin films gradually weakens with the increase of the film thickness. In addition, it can be observed from Fig. S3a that the  $\tan\delta$  gradually decreases as the thickness of the BZTS/HfO<sub>2</sub> thin films. Fig. S3b shows the temperature dependence of  $\epsilon_r$  and  $\tan\delta$  for the BZTS/HfO<sub>2</sub> thin films of different thicknesses. The results show that the BZTS/HfO<sub>2</sub> thin films with thickness of 415 nm has the best thermal stability.

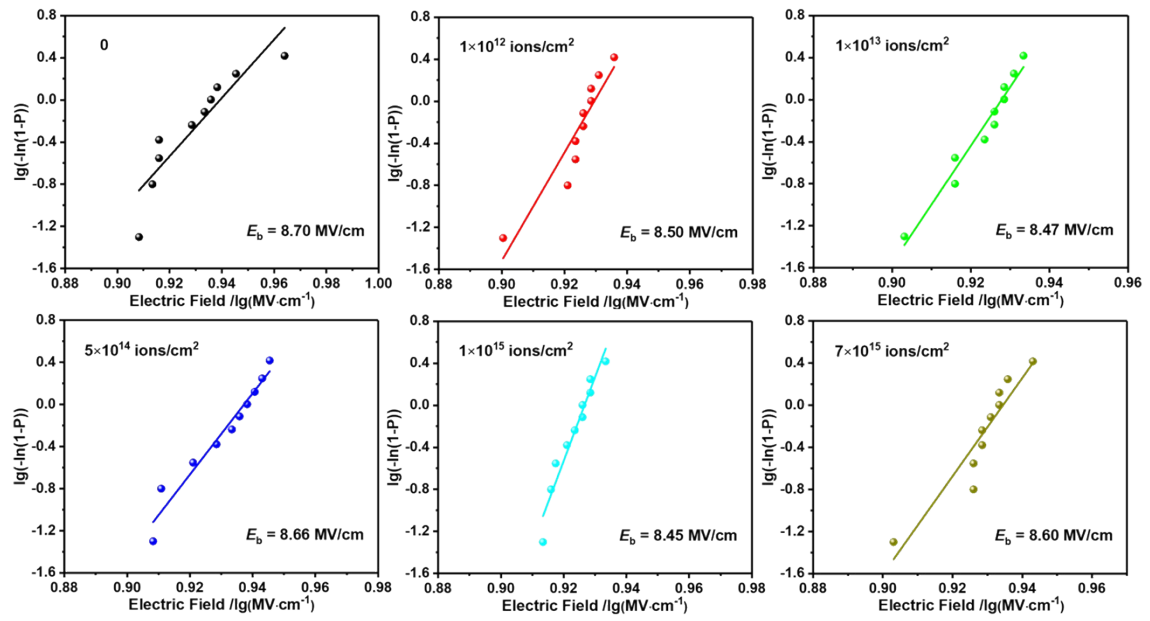


Fig. S4 After He<sup>+</sup> irradiation with different doses, the Weibull distribution and the fitting lines of  $E_b$  for the BZTS/HfO<sub>2</sub> thin film capacitors.

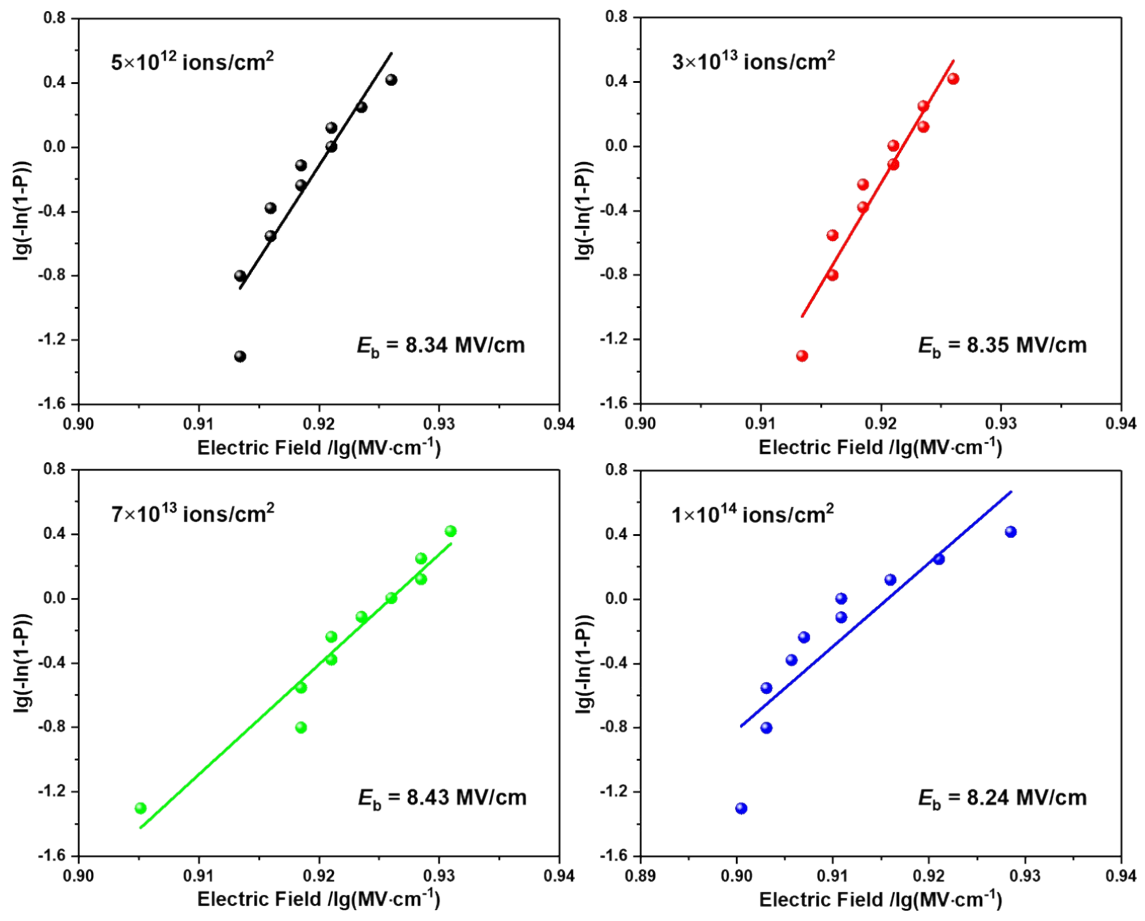


Fig. S5 After neutron irradiation with different doses, the Wei-bull distribution and the fitting lines of  $E_b$  for the BZTS/HfO<sub>2</sub> thin film capacitors.

## References

- 1 C. Neusel, G. A. Schneider, *J. Mech. Phys. Solids.*, 2014, **63**, 201-213.